C. R. Chimie 19 (2016) 1573–1579

Contents lists available at ScienceDirect

Comptes Rendus Chimie

www.sciencedirect.com

Full paper/Mémoire

Structural elucidation of silica present in kidney stones coming from Burkina Faso

Élucidation structurale de la silice présente dans des calculs rénaux prélevés au Burkina Faso

Arnaud Dessombz [a, b, *], Gérard Coulibaly [c], Brahima Kirakoya [c], Richard W. Ouedraogo [c], Adama Lengani [c], Stéphan Rouziere [b], Raphael Weil [b], Lise Picaut [b], Christian Bonhomme [d], Florence Babonneau [d], Dominique Bazin [b, d], Michel Daudon [e]

[a] *INSERM, UMR 1138, Laboratoire de physiopathologie orale moléculaire, Centre de recherche des Cordeliers, équipe Berdal, Université Paris-5, Université Paris-6, Université Paris-7, Paris, France*
[b] *CNRS, Laboratoire de Physique des Solides, Université Paris-11, 91405 Orsay cedex, France*
[c] *Service de néphrologie et hémodialyse, CHU Yalgado Ouédraogo, Ougadougou, Burkina Faso*
[d] *Sorbonne Universités, UPMC UNiversité Paris-6, ULR CNRS 7574, Laboratoire de chimie de la matière condensée de Paris (LCMCP), Collège de France, 11, place Marcelin-Berthelot, 75005 Paris, France*
[e] *AP-HP, Hôpital Tenon, Service d'explorations fonctionnelles, 4, rue de la Chine, 75970 Paris cedex 20, France*

ARTICLE INFO

Article history:
Received 5 December 2015
Accepted 28 June 2016
Available online 20 October 2016

Keywords:
Kidney stones
Opaline silica
Component
Urolithiasis
Burkina Faso
Structure

ABSTRACT

Hundred kidney stones obtained from the University Hospital of Ouagadougou (Burkina Faso) were finally characterized by a panel of complementary spectroscopic and diffraction tools. The most surprising result is the high occurrence of opaline silica as a component in these kidney stones. Opaline silica is a scarce mineral phase in renal calcification; however, we found that at least 48% of the stones had a detectable proportion of silica. SEM images demonstrate the presence of micrometric objects (of spheroidal shape) in close association with monohydrated calcium oxalate crystals. X-ray fluorescence, XRD and ^{29}Si solid state MAS NMR demonstrate unambiguously the presence of amorphous silica, whose composition is comparable to that of natural opals. As NMR is a local spectroscopic probe, other nuclei can be probed. We demonstrate that traces of aluminium are present in the kidney stones by using ^{27}Al solid state MAS NMR. These experiments may offer the first clues of pathological processes that are responsible for these stones.

Mots-clés:
Calculs rénaux
Silice opaline

RÉSUMÉ

Cent calculs rénaux obtenus du CHU de Ouagadougou (Burkina Faso) ont été caractérisés par une série d'outils spectroscopiques et de diffraction complémentaires. Le résultat le plus marquant a été la très haute prévalence de la silice opaline comme composant de ces

* Corresponding author.
E-mail address: arnaud.dessombz@crc.jussieu.fr (A. Dessombz).

http://dx.doi.org/10.1016/j.crci.2016.06.012

Composant
Lithiase urinaire
Burkina Faso
Structure

calculs. La silice opaline est un composant rare des calculs rénaux. Cependant, nous l'avons trouvée dans près de 48% des calculs, dans des proportions suffisantes pour être détectables par analyse infrarouge. Les images au MEB démontrent la présence d'objets micrométriques (de forme sphérique) en association intime avec des cristaux d'oxalate de calcium monohydraté. La fluorescence des rayons X, la diffraction des rayons X et la RMN du solide du ^{29}Si démontrent sans ambiguïté la présence de silice amorphe, de manière comparable au cas des opales naturelles. Comme la RMN est une sonde spectroscopique locale, d'autres noyaux peuvent être détectés. Nous avons ainsi démontré que des traces d'aluminium sont présentes dans les calculs rénaux étudiés en utilisant la RMN du solide du noyau ^{27}Al. Ces expériences peuvent offrir les premiers éléments de réponse concernant le processus pathologique conduisant à la formation de ces calculs.

1. Introduction

Renal lithiasis is a consequence of biocrystallization [1–5] of different chemical compounds in the urinary tract corresponding to various pathologies encompassing genetic disorders [4], infection [5], acquired metabolic diseases and most often metabolic risk factors related to dietary habits [6]. Among these relations with pathologies, the prevalence of calcium oxalate (CaOx) stones is associated with significant changes in the dietary habits in industrialized countries [7,8]. In contrast, the presence of silica in kidney stones is quite rare and often related to the administration of drugs [9–13]. None of the large series of stone analyses reported in the literature has identified silica among the chemical phases present in kidney stones.

Recently, a set of 100 consecutive kidney stones coming from the CHU of Ougadougou (Burkina Faso) has been analyzed following the classical analysis procedure based on morphologic examination combined with Fourier-transform infrared (FTIR) analysis [14]. In a significant number of these kidney stones (48%) [15], the presence of amorphous silica has been observed. Silica was present in the nucleus of 42 stones (42%) and was especially frequent in the core of stones from women (72.7% of cases). Moreover, while the content of silica is usually low, silica was the major component of 18% of the stones. Such unusual prevalence of silica in kidney stones has motivated an investigation through physical techniques in order to describe precisely the status of Si atoms.

We and other authors have already demonstrated in different studies the advantages of using physical methods to precisely characterize kidney stones and more generally pathological calcifications [16–18]. Among them, we can quote scanning and transmission electron microscopy (SEM, TEM) [19,20], in situ atomic force microscopy [21], X-ray and neutron scattering [22–24], atomic absorption spectrometry [25], infra-red and Raman vibrational spectroscopies [26–30], micro-computed tomography [31,32], fluorescence induced by X-ray or neutrons [33–35], Nuclear Magnetic Resonance [36–39] as well as techniques specific to synchrotron radiation [40–45].

In this paper, we gathered structural information on silica present in a set of selected kidney stones in order to assess its biological origin. For this purpose, we initially determined stone composition through FTIR experiments, confirmed the amorphous state of silica through X-ray scattering, underlined the presence of different elements through X-ray fluorescence and collected images of different kidney stones at the mesoscopic scale by SEM. Finally, valuable structural information regarding the silica phase was gathered through solid state NMR. This spectroscopic technique, which is a local probe in nature, can bring invaluable structural information regarding the environment of Si [46].

2. Materials and methods

2.1. Patients

We investigated 100 kidney stones collected after open surgery ($n = 99$) or spontaneous expulsion ($n = 1$) from the University Hospital of Ouagadougou (Burkina Faso). The patients were 85 adults (64 men aged 47.0 ± 18.5y and 22 women aged 39.1 ± 15.3y) and 14 children (10 boys aged 9.8 ± 4.7y and four girls aged 11.4 ± 5.5y). All participants, and legal tutors for minor children, gave their verbal consent for use of the material. Ethical approval for the study was obtained from the ethics committee of the Tenon Hospital.

2.2. FTIR (FTIR) spectroscopy

All the samples have been characterized by Fourier transform infrared (FTIR) spectroscopy. To do so, an FTIR spectrometer, Vector 22 (Bruker Optics, Champs-sur-Marne, France), was used according to the analytical procedure previously described [47,48]. Data were collected in the absorption mode between 4000 and 400 cm^{-1} with a resolution of 4 cm^{-1}.

2.3. Scanning electron microscopy (SEM)

A Zeiss SUPRA55-VP SEM was used for the observation of the microstructure [49]. This field-effect “gun” microscope (FE-SEM) operates at 0.5–30 kV. High-resolution observations were obtained by two secondary electron detectors: an in-lens SE detector and an Everhart-Thornley SE detector. To maintain the integrity of the samples, for both SEMs, measurements were taken without the usual deposits of carbon at the surface of the sample.

2.4. X-ray diffraction (XRD)

Phase identification and crystallinity of the dental mineral part were evaluated by X-ray diffraction. Experiments were carried out with a molybdenum rotating anode X-ray generator (RIGAKU RUH2R) coupled with multilayer W/Si optics delivering a focalized and monochromated ($\lambda = 0.711$ Å) X-ray beam of 800 μm × 1 mm size onto the sample. X-ray images were recorded with a MAR345 (@MAR Research) detector placed at of a distance of 200 mm from the sample. The acquisition time of each measurement was 30 mn. Diffraction diagrams were obtained by processing radial intensity integration of each image. Then positions of the diffraction peaks were compared with the reference files from the JCPDS database.

2.5. X-ray fluorescence (XRF)

X-ray fluorescence allows the precise determination of the elemental composition of the sample. Experiments were carried out with a molybdenum rotating anode X-ray generator (RIGAKU RU200) coupled with multilayer W/Si optics delivering a focalized and monochromated ($\lambda = 0.711$ Å) X-ray beam of 150 μm × 150 μm size. Fluorescence spectra were measured with an energy dispersive detector (SDD detector @Ketek), with a time acquisition of 1500s each. XRF analysis was performed with PyMca software [50].

2.6. NMR spectroscopy

^{29}Si and ^{27}Al SPE (Single Pulse Experiment) MAS NMR experiments were performed on a Bruker 300 AVANCE III spectrometers using 7 mm Bruker MAS probes (samples were packed in zirconia rotors). All experimental parameters including pulse flip angles, recycling delays, number of scans, $\{^1H\}$ decoupling schemes are presented in the caption of the corresponding figures. Chemical shifts were referenced towards TMS for ^{29}Si and $Al(NO_3)_3$, 1 mol L^{-1} in HNO_3, 1 mol L^{-1} for ^{27}Al. All spectra were fitted by using the DMFit software available free on the web [51,52].

3. Results

The starting point of this contribution is given by a set of photographs collected on kidney stones containing various proportions of silica. In Fig. 1, both of these kidney stones display a concentric structure, either as well organized layers with radiating crystals (Fig. 1a), or as more diffuse layers (Fig. 1b and c). In Fig. 1a, the white core is mainly made of opaline silica (OPA) while the dark-brown inner and surrounding layers are pure calcium oxalate monohydrate. In Fig. 1b, white layers are mainly composed of OPA with various proportions of whewellite (calcium oxalate monohydrate, COM) and proteins while brown layers are mainly made of COM with minor proportions of OPA. By contrast with the stone shown in Fig. 1a, where OPA was only found in the nucleus, the stone of Fig. 1b contained

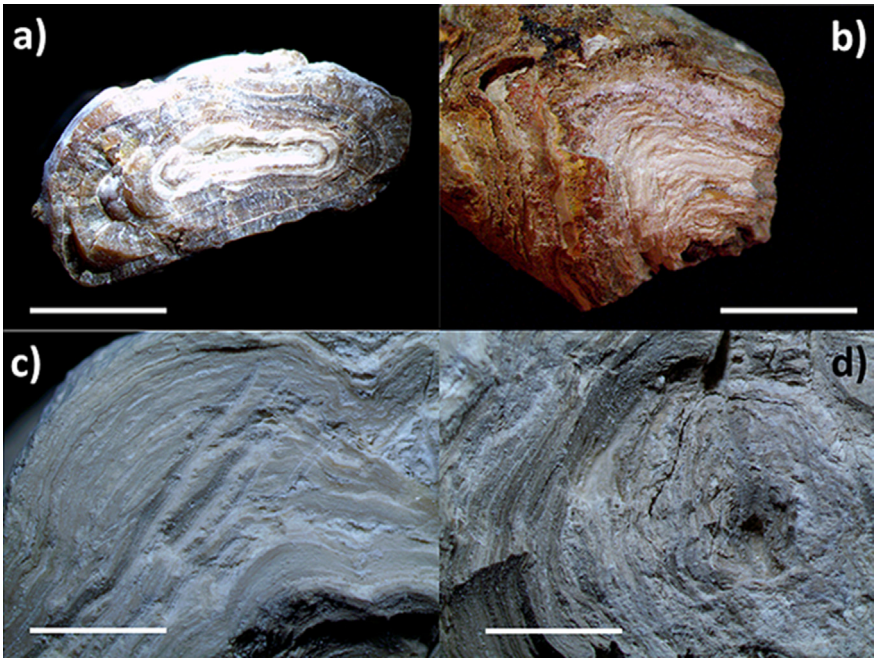

Fig. 1. Photographs of various stones containing OPA. (a) Cross-section of the stone T67317, made of a mixture of COM (90%), OPA (7%) and proteins (3%). The white core is mainly composed of OPA; (b) cross-section of the stone T67309. The OPA content was higher than in the sample T67317 and was distributed through the core and the various layers, mixed with COM. The global stone composition was COM (72%) + OPA (15%) + proteins (10%) + ammonium hydrogen urate (3%); (c) and (d) cross-section of the stone T67974 mainly made of OPA (81%), mixed with proteins (13%) and COM (6%). Peripheral layers are shown in figure (c) and the stone core is shown in figure (d). The stone core contained essentially OPA with small proportions of proteins and traces of COM. (white bar: 5 mm).

OPA in the core and inner or peripheral layers as well. Moreover, the core contained also small proportions of ammonium hydrogen urate, which suggests that the precipitation of OPA occurred in alkaline (or poorly acidic) urine. Finally, in Fig. 1c, a stone mostly composed of OPA (81%) mixed with proteins (13%) and COM (6%) revealed diffuse irregular layers (see Fig. 2).

These observations at the macroscopic and mesoscopic (under micron) scales have been completed by FTIR experiments [15]. Among the different locations of the stones within the urinary tract, there was no difference between stone containing, or not, OPA. For example, stones that contained OPA were removed from the upper urinary tract in 69% of cases versus 63.5% of cases in the absence of OPA within the stone. Of interest, we found differences regarding the gender of the patient: OPA-containing stones were significantly more frequent in females than in males (69.2% vs 40.5%, $p = 0.02$). The content of OPA ranged from only 2% up to 82% of the stone mass. For 17% of the stones (12.2% for men, 30.8% for women) silica was the major component. Regarding the nucleus of the stones, silica was the major component for 39% of the stones (32.4% for men, 57.7% for women) which indicate that OPA was often present at the nucleation process (see Fig. 3).

The chemical composition as measured by FTIR spectroscopy has been completed by X-ray fluorescence in order to obtain the elementary composition. In Fig. 5, typical X-ray fluorescence spectra have been plotted. The different contributions of Si ($K\alpha = 1.730$ KeV), S ($K\alpha = 2.31$ KeV), Ar ($K\alpha = 2.96$ KeV), Ca ($K\alpha = 3691$ eV, $K\beta = 4012$ eV) are visible. The presence of Ar is related to the experimental conditions. The presence of a small amount of Al ($K\alpha = 1.49$ KeV) is also pointed through a feature in the fluorescence signal of Si. Interestingly, the fact that X-ray fluorescence shows the presence of Al and Si seems to indicate that aluminosilicate phases are present in these kidney stones.

Fig. 6 shows powder XRD patterns measured for different kidney stones. On the scattering patterns, we can see clearly a set of well-defined X-ray diffraction peaks (at $2\theta^\circ = 14.75^\circ$, 24.18°, 29.99°) corresponding to the whewellite in line with its crystallographic structure (monoclinic $P2_1/c$; $a = 6.316$ Å, $b = 14.541$ Å, $c = 10.116$ Å) [53]. Moreover, an additional broad component is associated with silica. Such large peak indicates an amorphous structure for the silica. The intensity of this large diffraction peak is related to the content of silica as measured by FTIR spectroscopy (see Fig. 4).

These stones were further investigated by ^{29}Si and ^{27}Al solid state NMR (under MAS, Magic Angle Spinning). A typical ^{29}Si MAS spectrum (decoupled from protons) is presented in Fig. 7. Such a spectrum can be fully interpreted by taking into account Q^2, Q^3 and Q^4 units (Q^2: $Si(OH)_2(OSi)_2$, Q^3: $Si(OH)(OSi)_3$, Q^4: $Si(OSi)_4$ [54]. It is comparable to those obtained for natural opals [55]. Q^2 species correspond to a very minor contribution.

The ^{27}Al MAS NMR spectra are presented in Fig. 8. Considering the long acquisition time (several hours) for such a sensitive NMR nucleus, it is clearly demonstrated here that traces of aluminum are actually detected. One major signal (with maximum intensity at $\delta \approx 55$ ppm) is observed. It corresponds essentially to 4-fold coordinated species but 5-fold coordinated nuclei cannot be excluded. A test spectrum corresponding to an empty rotor is presented in the inset in Fig. 8. It demonstrates unambiguously that the signal centered ≈ 55 ppm is characteristic of the sample. The much less intense signal at ≈ 0 ppm can be attributed partly to the rotor background [56]. It has to be

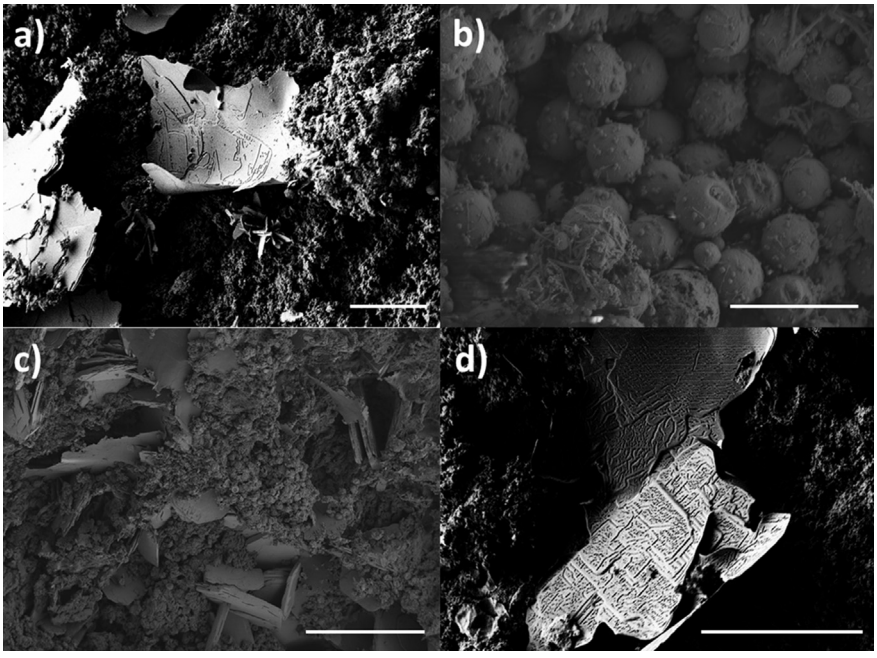

Fig. 2. (a,b) SEM photographs of a kidney stone containing 58% of OPA and 25% of COM: parts of the sample which contain mainly COM (a) or mainly silica (b); (c) SEM photograph of a kidney stone containing 82% of OPA; (d) SEM photographs of a kidney stone containing 20% of OPA. (white bar: 10 μm).

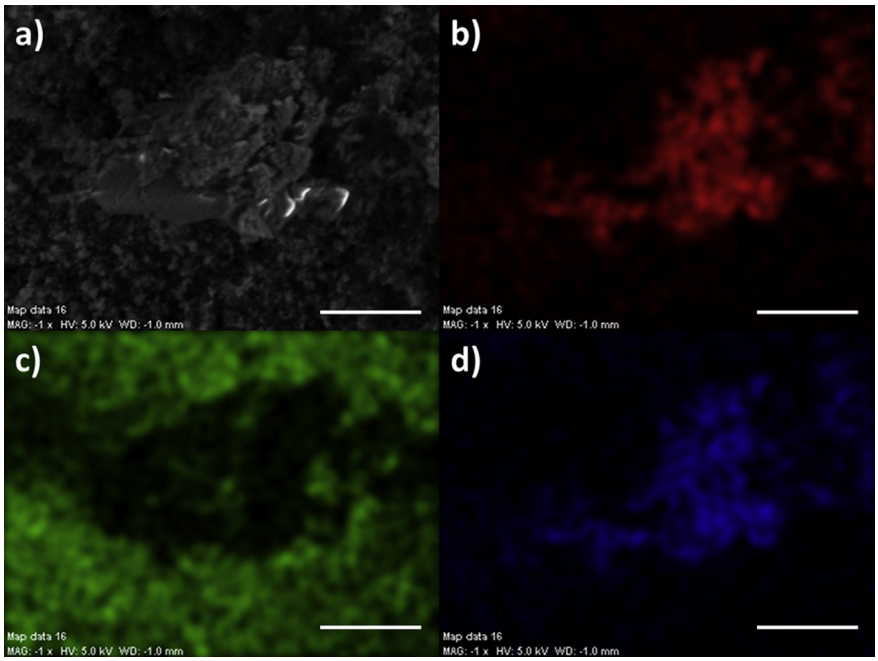

Fig. 3. Spatial repartition of different elements measured through EDX of a kidney stone containing 65% of OPA and 25% of COM (a) SEM photograph, (b) Ca distribution, (c) Si distribution, (d) C distribution. (white bar: 10 μm).

mentioned here that a similar ^{27}Al MAS spectrum was obtained for tabasheer, an opal of plant origin (about 1–2wt % in aluminum) [57]. In this particular case, it is assumed that most of the Al atoms are part of the silicate network.

4. Discussion

The influence of silica on the kidney function has been investigated by different authors [56,58]. For example, S. Vupputuri et al. [59] found a positive relationship between occupational silica exposure and CKD.

The presence of silica in kidney stones has been reported in different animals [60,61] but is quite rare in human. In that case, as previously mentioned, the presence of silica is related to drug administration [9,12,13]. Information regarding a possible drug origin for the kidney stones selected in this study was not available for all patients. However, several patients who produced stones containing OPA denied any kind of medication. Moreover, as underlined by Raghuvanshi et al. [62], even if occupational exposure to silica dust has been increasing the possible risk of varieties of pathologies, no case of kidney stones made of silica has been reported.

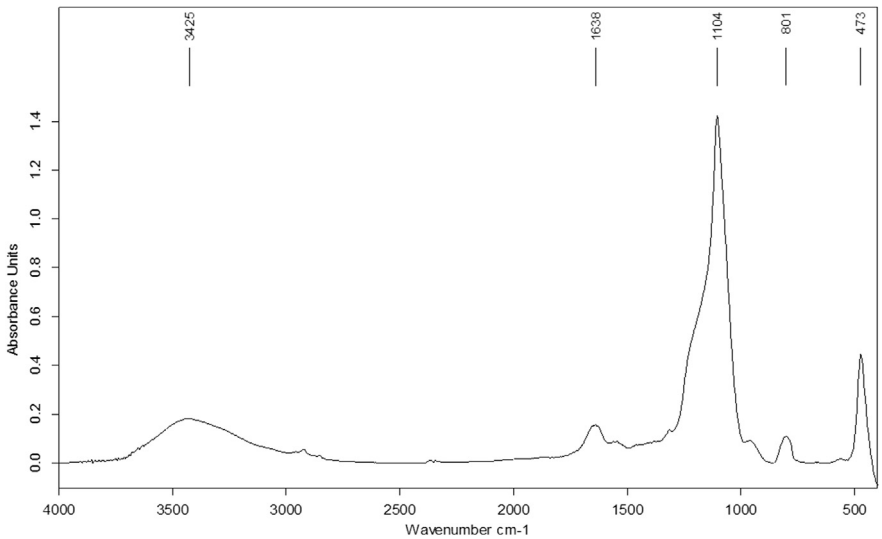

Fig. 4. Typical OPA FTIR spectrum collected for a kidney stone containing a high content of silica. The black arrow indicates a very small proportion of COM.

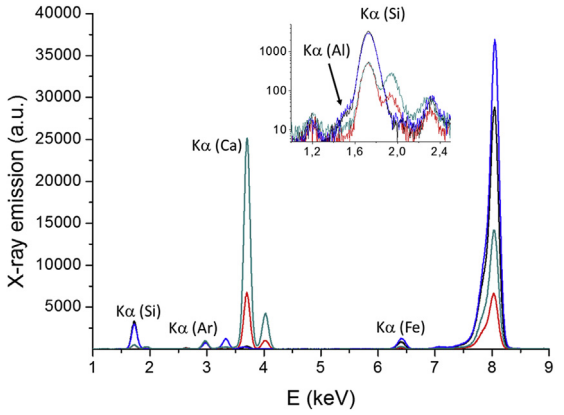

Fig. 5. Typical X-ray fluorescence spectrum collected for selected samples. We can see clearly the contributions of Si (Kα = 1.73 keV), S (Kα = 2.31 keV), Ar (Kα = 2.96 keV), Ca (Kα = 3.69 keV, Kβ = 4.01 keV).

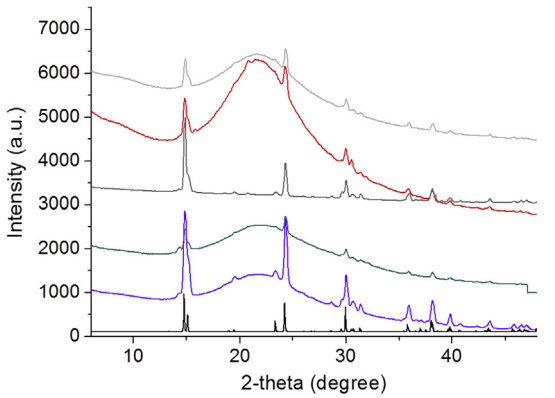

Fig. 6. X-ray scattering diagram of selected samples. A broad X-ray scattering peak corresponding to silica superimposed to whewellite peaks (pure whewellite: black solid line).

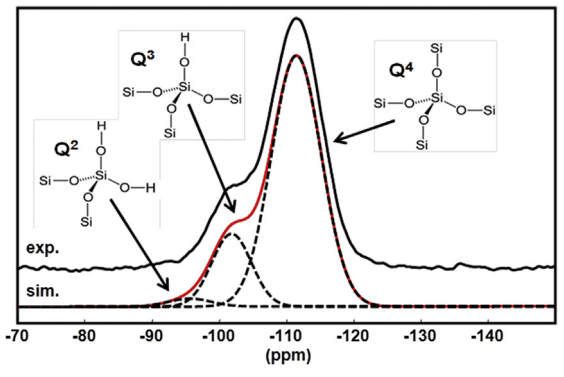

Fig. 7. ^{29}Si SPE (single pulse experiment) MAS NMR spectrum of the kidney stone. B_0 = 7 T, 7 mm MAS probe, $\nu_{rot.}$ = 5 kHz, $t_{90°}(^{29}Si)$ = 5.0 μs, pulse angle = 30°, {^{1}H} SPINAL-64 high power decoupling, recycling delay: 600 s, number of scans: 248 (≈41 h). In black: experimental spectrum. In red: deconvolution of the exp. spectrum in Q^2, Q^3 and Q^4 units using DMFit [51,52] (see text).

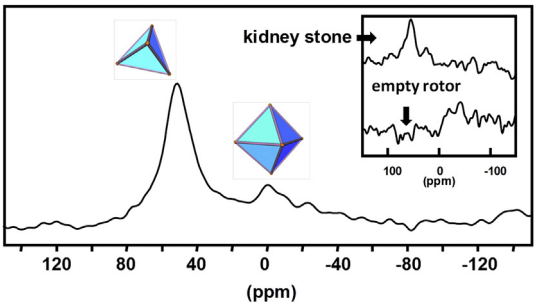

Fig. 8. ^{27}Al SPE (single pulse experiment) MAS NMR spectrum of a representative kidney stone (same sample studied by ^{29}Si MAS). B_0 = 7 T, 7-mm MAS probe, $\nu_{rot.}$ = 5 kHz, selective excitation of the central transition checked on YAG garnet, recycling delay: 1 s, number of scans: 54,000 (≈15 h). The characteristic zones for 4-and 6-fold ^{27}Al resonances are indicated as a guideline. Inset: ^{27}Al SPE MAS NMR spectrum of an empty rotor and of the kidney stone sample. Acquisition time: 2 h.

^{29}Si SPE MAS NMR is a suitable tool of investigation for the characterization of amorphous silicates and aluminosilicates. The amorphous nature of the silica present in the stones is clearly demonstrated by the broad Q^2, Q^3 and Q^4 resonances observed in Fig. 7. The broadening of the lines reflects mainly the distributions of isotropic ^{29}Si chemical shifts, due to variations in bond lengths and bond angles. We stress here that ^{29}Si SPE MAS NMR can be considered as quantitative as soon as full relaxation of the spin system is explicitly taken into account. The $T_1(^{29}Si)$ longitudinal relaxation times for the $Q^2 + Q^3$ and Q^4 units were estimated by saturation-recovery experiments (not shown). The recovery curves were fitted with stretched exponentials following recent work by Stebbins et al. [63,64]. From the fitted curves, the ratio $Q^4/(Q^2 + Q^3)$ is estimated to 86/14. The deconvolution of the experimental ^{29}Si MAS spectrum (Fig. 7) leads to 79/21. In other words, the relaxation delay used here (i.e. 600 s) is still not sufficient to ensure full relaxation of the Q^4 units. The detailed study of the ^{29}Si relaxation will be presented in a future work.

The presence of traces of aluminium in urinary stones is demonstrated as well by ^{27}Al SPE MAS NMR. The amount of aluminium in the samples is very limited; consequently, eventual Al impurities in the NMR rotors have to be considered (see the inset in Fig. 8). The Al atoms are mostly 4-fold coordinated (5-fold coordination cannot be strictly ruled out as experiments were performed in a unique magnetic field). The associated ^{27}Al broad resonance is compatible with aluminium species found in aluminosilicates [54].

In the case of ^{27}Al, the broadening of the line can be assigned to both distributions of isotropic ^{27}Al chemical shifts *and* quadrupolar constants (as $I = 5/2$ for ^{27}Al). Both contributions could be unambiguously separated by variable field NMR experiments (as second-order quadrupolar effects are inversely proportional to B_0) and subsequent fitting of the obtained line shapes. Theoretical models for the distributions are available in DMFit [51,52].

The quantification of the aluminium content by using an internal reference (such as alun, $KAl(SO_4)_2 \cdot 12H_2O$) is currently under investigation. It has to be mentioned here that even lower amounts of aluminum could be detected by combining advanced solid state NMR techniques, such as

WURST excitation [65] and QCPMG [66] acquisition of the spectra. Indeed, it has been demonstrated that such a combination of specific NMR techniques could increase dramatically the signal/noise ratio of NMR experiments related to quadrupolar nuclei by several orders of magnitude [67].

5. Conclusion

Unusual amounts of silica have been identified through FTIR spectroscopy in a set of 100 urinary stones coming from the Hospital of Ouagadougou (Burkina Faso). X-ray scattering as well as NMR measurements indicate the amorphous character of silica. Moreover, solid state NMR is able to characterize the presence of elemental traces such as aluminium. It is suggested that the origin of aluminium could be a mixture with silicon derivatives in the form of aluminosilicates.

Acknowledgements

Arnaud Dessombz was supported by grants “Once Upon a Tooth” IDEX (grant number: ANR-11-IDEX-0005-02) and ANR Nanoshap (grant number: ANR-09-BLAN-0120-02).

References

[1] P.N. Rao, G.M. Preminger, J.P. Kavanagh (Eds.), Urinary Tract Stone Disease, Springer-Verlag Ltd, London, 2011.
[2] J. Gómez-Morales, G. Falini, J.M. García-Ruiz, Handbook of Crystal Growth, 2nd ed., 2015, pp. 873–913.
[3] H. Singh Bagga, Th. Chi, J. Miller, M.L. Stoller, Urologic Clin. N. Am. 40 (2013) 1.
[4] M. Daudon, P. Jungers, D. Bazin, N. Engl. J. Med. 359 (2008) 100.
[5] R. Flannigan, W.H. Choy, B. Chew, D. Lange, Nat. Rev. Urol. 11 (2014) 333.
[6] J.-P. Haymann, M. Daudon, M. Normand, A. Hoznek, P. Méria, O. Traxer, les membres CLAFU, Progrès Urol. 24 (2014) 9.
[7] E.N. Taylor, G.C. Curhan, Nephron Physiol. 98 (2004) 55.
[8] C.Y. Pak, C.V. Odvina, M.S. Pearle, K. Sakhaee, R.D. Peterson, J.R. Poindexter, L.J. Brinkley, Kidney Int. 68 (2005) 2264.
[9] D.A. Levinson, P.R. Crocker, S. Banim, D.M. Wallace, Lancet 1 (1982) 704.
[10] J. Irani, B. Doré, D. Bon, T. Hauet, J. Aubert, Prog. Urol. 2 (1992) 290.
[11] M. Augusti, J.C. Mikaelian, H. Monsaint, D. Brin, M. Daudon, Prog. Urol. 3 (1993) 812.
[12] T. Ulinski, J.-F. Sabot, I. Bourlon, P. Cochat, Eur. J. Pedia 163 (2004) 239.
[13] J.E. Flythe, J.F. Rueda, M.K. Riscoe, S. Watnick, Am. J. Kidney Dis. 54 (2009) 127.
[14] M. Daudon, C.A. Bader, P. Jungers, Scanning Microsc. 7 (1993) 1081.
[15] A. Dessombz, B. Kirakoya, G. Coulibaly, R.W. Ouedraogo, L. Picaut, R. Weil, D. Bazin, M. Daudon, Urology 86 (2015) 1090.
[16] D. Bazin, M. Daudon, C. Combes, C. Rey, Chem. Rev. 112 (2012) 5092.
[17] D. Bazin, J.-P. Haymann, E. Letavernier, J. Rode, M. Daudon, La Presse médicale 43 (2014) 135.
[18] M.L. Giannossi, J. X-ray Sci. Technol. 23 (2015) 401.
[19] A.V. Kustov, A.A. Shevyrin, A.I. Strelnikov, P.R. Smirnov, V.N. Trostin, Urol. Res. 40 (2012) 205.
[20] A.P. Evan, Pediatr. Nephrol. 25 (2010) 831.
[21] S. Li, W. Zhang, L. Wang, Cryst. Growth Des. 15 (2015) 3038.
[22] J. Prywer, A. Torzewska, T. Płocinski, Urol. Res. 40 (2012) 699.
[23] D. Bazin, M. Daudon, G. André, R. Weil, E. Véron, G. Matzen, J. Appl. Crystallogr. 47 (2014) 719.
[24] D. Bazin, G. André, R. Weil, G. Matzen, E. Véron, X. Carpentier, M. Daudon, Urology 79 (2012) 786.
[25] M. Siojewski, B. Czerny, K. Safranow, M. Drosdzik, A. Pawlik, K. Jakubowska, M. Olszewska, A. Goiab, E. Byra, D. Chlubek, A. Sikorski, Urol. Res. 37 (2009) 317.
[26] Z. Jing, W. GuoZeng, J. Ning, Y. JiaWei, G. Yan, Y. Fang, Urol. Res. 38 (2012) 111.
[27] M. Pucetaite, S. Tamosaityte, A. Engdahl, J. Ceponkus, V. Sablinskas, P. Uvdal, Cent. Eur. J. Chem 12 (2014) 44.
[28] T.N. Moroz, N.A. Palchik, A.V. Dar'in, Nucl. Instr. Meth. Phys. Res. A 603 (2009) 141.
[29] J. Tonannavar, G. Deshpande, J. Yenagi, S.B. Patil, N.A. Patil, B.G. Mulimani, Spectrochim. Acta Part A 154 (2016) 20.
[30] D. Bazin, M. Daudon, Ann. Biol. Clin. 73 (2015) 517.
[31] J.C. Williams, J.A. McAteer, A.P. Evan, J.E. Lingeman, Urol. Res. 38 (2010) 477.
[32] J. Kaiser, M. Hola, M. Galiova, K. Novotny, V. Kanicky, P. Martinec, J. Sicucka, F. Brun, N. Sodini, G. Tromba, L. Mancini, L. Koristkova, Urol. Res. 39 (2011) 259.
[33] D. Bazin, P. Chevallier, G. Matzen, P. Jungers, M. Daudon, Urol. Res. 35 (2007) 179.
[34] C.A. Pineda-Vargas, M.E.M. Eisa, A.L. Rodgers, Appl. Radiat. Isotopes 67 (2009) 464.
[35] B. Hannache, A. Boutefnouchet, D. Bazin, M. Daudon, E. Foy, S. Rouzière, A. Dahdouh, Progrès Urol. 25 (2015) 22.
[36] D.G. Reid, G.J. Jackson, M.J. Duer, M.L. Rodgers, J. Urology 185 (2011) 725.
[37] H. Colas, L. Bonhomme-Coury, C. Coelho Diogo, F. Tielens, F. Babonneau, C. Gervais, D. Bazin, D. Laurencin, M.E. Smith, J.V. Hanna, M. Daudon, C. Bonhomme, CrystEngComm. 15 (2013) 8840.
[38] C. Bonhomme, C. Gervais, D. Laurencin, Prog. Nucl. Magnetic Reson. Spectrosc. 77 (2014) 1.
[39] C. Martineau, Solid State Nucl. Magn. Reson. 63–64 (2014) 1.
[40] D.E. Fleming, A. Van Riessen, M.C. Chauvet, P.W.K. Grover, B. Hunter, W. Van Bronswijk, R.L. Ryall, J. Bone Min. Res. 18 (2003) 1282.
[41] A.I. Ancharov, A.I. Nizovskii, S.S. Potapov, T.N. Moiseenko, I.V. Feofilov, Bull. Russ. Acad. Sci. Phys. 71 (2007) 653.
[42] J. Siritapetawee, W.X. Pattanasiriwisawa, J. Syn. Rad. 15 (2008) 158.
[43] X. Carpentier, D. Bazin, P. Jungers, S. Reguer, D. Thiaudière, M. Daudon, J. Synchrotron Rad. 17 (2010) 374.
[44] A. Dessombz, D. Bazin, P. Dumas, C. Sandt, J. Sule-Suso, M. Daudon, PLoS One 6 (2011) e28007.
[45] F. Blanco, P. Ortiz-Alías, M. López-Mesas, M. Valiente, J. Biophot. 8 (2015) 457.
[46] C. Bonhomme, C. Coelho, N. Baccile, C. Gervais, T. Azaïs, F. Babonneau, Acc. Chem. Res. 40 (2007) 738.
[47] L. Estepa, M. Daudon, Biospectroscopy 3 (1997) 347.
[48] N. Quy Dao, M. Daudon, Infrared and Raman Spectra of Calculi, Elsevier, Paris, 1997.
[49] F. Brisset, M. Repoux, J. Ruste, F. Grillon, F. Robaut, Microscopie électronique à balayage et Microanalyses, EDP Sciences, 2009, ISBN 978-2-7598-0082-7.
[50] V.A. Solé, E. Papillon, M. Cotte, Ph Walter, J. Susini, Spectrochim. Acta Part B 62 (2007) 63–68.
[51] D. Massiot, F. Fayon, M. Capron, I. King, S. Le Calvé, B. Alonso, J.O. Durand, B. Bujoli, Z. Gan, G. Hoatson, Magn. Reson. Chem. 20 (2002) 70.
[52] http://www.cemhti.cnrs-orleans.fr.
[53] M. Daudon, D. Bazin, G. André, P. Jungers, A. Cousson, P. Chevallier, E. Véron, G. Matzen, J. Appl. Crystallogr. 42 (2009) 109.
[54] K.J.D. Mackenzie, M.E. Smith, Multinuclear Solid-state NMR of Inorganic Materials, Pergamon Materials Series, 2002.
[55] L.D. Brown, A.S. Ray, P.S. Thomas, J. Non Cryst. Solids 332 (2003) 242.
[56] J. Klinowski, C.-F. Cheng, J. Sanz, J.M. Rojo, A.L. Mackay, Phil. Mag. 77 (1998) 201.
[57] P. Stratta, C. Canavese, A. Messuerotti, I. Fenoglio, B. Fubini, J. Nephrol. 14 (2001) 228.
[58] S. Fenwick, J. Main, Lancet 356 (2000) 913.
[59] S. Vupputuri, C.G. Parks, L.A. Nylander-French, A. Owen-Smith, S.L. Hogan, D.P. Sandler, Ren. Fail. 34 (2012) 40.
[60] J. Angel-Caraza, I. Diez-Prieto, C.C. Pérez-Garcia, M.B. Garcia-Rodriguez, Urol. Res. 38 (2010) 201.
[61] H.M. Syme, Arab J. Urology 10 (2012) 230.
[62] S. Raghuvanshi, S. Shrivastava, S. Johri, S. Shukla, J. Trace Elem. Med. Biol. 26 (2012) 205.
[63] J.F. Stebbins, J.R. Smyth, W.R. Panero, D.J. Frost, Am. Mineral. 94 (2009) 905.
[64] S.M. Chemtob, G.R. Rossman, J.F. Stebbins, Am. Mineral. 97 (2012) 203.
[65] L.A. O'Dell, R.W. Schurko, Chem. Phys. Lett. 464 (2008) 9.
[66] R. Siegel, T.T. Nakashima, R.E. Wasylichen, Concepts Magn. Reson., Part A 26A (2005) 62.
[67] C. Bonhomme, C. Gervais, N. Folliet, F. Pourpoint, C. Coelho Diogo, J. Lao, E. Jallot, J. Lacroix, J.-M. Nedelec, D. Iuga, J.V. Hanna, M.E. Smith, Y. Xiang, J. Du, D. Laurencin, J. Am. Chem. Soc. 134 (2012) 12611.